

BUILDING DAMAGE SCENARIOS BASED ON EXPLOITATION OF HOUSNER INTENSITY DERIVED FROM FINITE FAULTS GROUND MOTION SIMULATIONS

Leonardo Chiauzzi¹, Angelo Masi¹, Marco Mucciarelli¹, Marco Vona¹, Francesca Pacor², Giovanna Cultrera², Frantisek Gallovič^{3,4} and Antonio Emolo³.

1. Department of Structures, Geotechnics and Engineering Geology, University of Basilicata, Potenza, Italy.
2. Istituto Nazionale di Geofisica e Vulcanologia, via Bassini 15, 20133 Milan, Italy.
3. Dipartimento di Scienze Fisiche, Università “Federico II”, Naples, Italy.
4. Department of Geophysics, Charles University, Prague, Czech Republic.

Corresponding author: Leonardo Chiauzzi, e-mail leonardochiauzzi@hotmail.it.

Keywords: damage scenario, building vulnerability, Housner intensity, EMS macroseismic intensity, finite faults ground motion simulations.

Abstract

In this paper earthquake damage scenarios for residential buildings (about 4200 units) in Potenza (Southern Italy) have been estimate adopting a probabilistic approach that involves complex source models, site effects, building vulnerability assessment and damage estimation through Damage Probability Matrices (DPMs). The studied area experienced several destructive earthquakes in historical and recent times. Several causative faults of single seismic events, with magnitude up to 7, are known to be close to the town. A seismic hazard approach based on finite faults ground motion simulation techniques has been used to identify the sources producing the maximum expected ground motion at Potenza and to generate a set of ground motion time histories to be used for building damage scenarios. Additionally, site effects, evaluated in the framework of the DPC-INGV S3 project through amplification factors of Housner intensity (I_H), have been combined with the bedrock values provided by hazard assessment. Furthermore, a new relationship between I_H and macroseismic intensity in terms of EMS98 has been developed. This relationship has been used to convert the Probability Density Functions (PDFs) for I_H obtained from synthetic seismograms and convolved by the site effects coefficients into PDFs for EMS98 intensity. Finally, the DPMs approach has been applied to estimate the damage levels of the residential buildings in the urban area of Potenza.

1. Introduction

Increasing urbanization, inadequate infrastructures and poorly engineered houses, as well as environmental degradation, are the main causes of human and economic losses during an earthquake (Khater *et al.*, 2003). These aspects and the consequent need for seismic prevention policies, have prompted the scientific community to develop suitable methodologies aimed at assessing and managing the earthquake risk. In this way, the setting up of both post-event emergency plans and prevention activities are the main tools for a medium-to-long term mitigation policy. An important step in achieving this objective, that is also required in the management of other natural risks, is the definition of the most probable damage scenarios. In an urban area, affected by an earthquake, scenarios are firstly related to the building damage assessment. For any given earthquake potentially hazardous for the selected area, the key elements needed for preparing building damage scenarios are the

definition of expected ground motion at bedrock, the seismic local amplifications due to site effects and the vulnerability assessment of involved buildings.

In the past times, several studies regarding earthquake loss scenarios, at different levels of refinement, have been carried out. To this end, several international projects, such as RISK-UE (Mouroux & Le Brun, 2006), LESSLOSS (Calvi & Pinho, 2004), ENSeRVES (Dolce *et al.*, 2002), and RADIUS (1999), have been developed. Particularly, in Italy, a great deal of interest has been raised by the Catania project (Faccioli *et al.*, 1999), where a comprehensive assessment of earthquake hazard, seismic microzonation and vulnerability of ordinary buildings and lifelines has been carried out. Recently, prompted by the need of operative procedures for the estimation of seismic risk at urban scale, the Italian Civil Protection and the National Institute of Geophysics and Volcanology, funded the S3 Project “*Shaking and damage scenarios in area of strategic and/or priority interest*”. In the framework of this Project, the town of Potenza was selected as a test site, considering the existing large data-set of building vulnerability and the local site conditions that can be considered as representative for most of the villages in the southern Apennines. The city (70,000 inhabitants), located in Basilicata region, Southern Italy, is classified as a high seismicity zone according to the current Italian Seismic Zonation (OPCM, 2003; NTC08, 2008). Indeed, the area around Potenza was affected by several destructive earthquakes in historical times (e.g., 1273, I_0 =VIII-IX MCS; 1561, I_0 =X; 1694, I_0 =XI; 1826, I_0 =IX; 1857, I_0 =XI). A number of individual sources, located at minimum distance of 20 km from the city with magnitude up to 7 can be identified. Other seismogenic faults have been recognized very close to the city, characterized by larger focal depth and smaller dimension, generating events with magnitude up to 5.7 (1990 Potenza earthquake, Azzara *et al.*, 1993).

In seismic risk management, scenarios can refer to different kinds of damage and losses, such as damage to constructions (buildings, bridges, etc.), casualties, economic losses due to interruption of activities, social losses, etc. (Dolce *et al.*, 2003). In this paper, damage scenarios relevant to residential buildings in the urban area of Potenza town are presented, that have been prepared following a multidisciplinary approach encompassing seismology and earthquake engineering. Usually, in studies at urban scale, the hazard models and the damage estimations are developed separately and they interact only during the generation of the seismic scenario. Contrarily, in this work, engineering and seismological analyses have been considered together and interacting from the beginning. The definition of the bedrock shaking scenarios and local amplifications have been carried out by choosing ground motion parameters which are well correlated to the seismic behaviour of building structures, and thus particularly suitable for the preparation of damage scenarios. To this regard, usually, in earthquake engineering design as well as in earthquake damage and/or loss models, peak ground acceleration (PGA) and peak ground velocity (PGV) are selected to define seismic intensity. But, while PGV is better related to the input energy (Ambraseys, 1974) and then it could be used as representative of seismic potential damage, PGA cannot be considered as an effective estimator of the potential damage of a ground motion (Masi, 2003; Masi *et al.*, 2010). Generally, the peak parameters as PGA and PGV are not very usable in the framework of damage scenario because they do not account for the earthquake duration, dominant frequency or seismic shaking energy. Moreover, their correlation with structural damage of buildings is very poor when compared with integral seismic parameters related to the dynamic response of structures. Masi *et al.* (2010), through non linear dynamic analyses performed on some typical reinforced concrete buildings, concluded that the Housner Intensity (I_H ; Housner, 1952) is the most effective parameter to correlate the severity of seismic events with building structural damage. Moreover, many authors (Pergalani *et al.*, 1999; Decanini *et al.*, 2002; Marcellini *et al.*, 2004) have also proposed I_H as a parameter which can represent better than PGA, PGV and Arias Intensity (Arias, 1970), the severity of earthquake ground motion. Then, in this study, the Housner Intensity associated with the ground motion signals to take into account the severity of earthquake shaking scenarios, has been used.

2. Methodology

The prediction of ground motions associated with future moderate-to-large earthquakes is a leading and complex problem in earthquake engineering analysis and it requires, as seismic input, a reliable and complete characterization of ground motion both in time and frequency domains (McGuire, 2001; McGuire, 1995; Chapman, 1995; Bazzurro & Cornell, 1999). Seismic hazard analysis for damage scenario can be estimated following both probabilistic (PSHA) and deterministic (DSHA) approaches (Cornell, 1968; Reiter, 1990; McGuire, 1995; Convertito *et al.*, 2006). The choice of the method to be used to perform hazard assessment is not simple, since both have advantages and disadvantages (McGuire, 1995; Bommer, 2002) and it depends on the purpose of the study and on the level of knowledge of the area of interest from the seismological point of view. In general, PSHA is largely applied in regions where information about seismogenic structures is poor or not available for the application of DSHA (Convertito *et al.*, 2006). For high-seismicity regions, deterministic approach, including physical description of both earthquake source and seismic waves propagation, may be particularly effective to provide a more realistic and accurate prediction of the ground motion. Therefore, the problem of performing a DSHA study at Potenza is related to the estimation of the ground motion produced by different seismogenic faults and, then, to the selection of procedures aimed at managing the available results in order to provide seismic input to be used for damage scenarios. It is worth noting that in the present study “deterministic” refers only to the a priori choice of seismogenic sources and anelastic attenuation parameters. The damage at the site is then estimated considering the probability of different rupture scenarios, fault slip distribution, slip velocity, rupture velocity, nucleation point, convolution with site effects, conversion between ground motion parameters and damage estimation modeling. The expected ground motions at bedrock are generally computed adopting physics-based methods, including kinematic description of an extend fault (Zollo *et al.*, 1997; Hartzell *et al.*, 1999 and references therein; Mai & Beroza, 2003; Pacor *et al.*, 2005; Gallovič & Brokešová, 2007). These models can be employed to capture the essential properties of the ground motion related to the variation of source parameters, such as rupture velocity, the final slip distribution over the fault plane, and the hypocenter location. In this way, complex source effects, like, for instance, ground motion amplification due to forward directivity, are taken into account. Furthermore, it is possible to consider combinations of source kinematic parameters related to the activation of specific seismogenic faults in order to generate a large number of synthetic time series at bedrock (Emolo & Zollo, 2001). The dataset of synthetic seismograms as well as the corresponding distribution of strong motion parameters, especially in regard to engineering requests, is then used to evaluate the seismic input needed for preparing the damage scenario.

Furthermore, observation of damage distributions from past seismic events shows that the influence of amplification related to local site effects needs to be considered when preparing a damage scenario. Also in this case, in order to deal coherently to a multidisciplinary perspective, the methodology needed to quantify seismic local amplifications has to be defined by taking into account the adopted building Damage Estimation Models (DEMs). Most recent trends in building vulnerability and damage estimation make use of analytical and mechanical models essentially based on the evaluation of dynamic response of tested structures and on the comparison between demand and capacity on the base of spectral response curves (e.g., Calvi *et al.*, 2006 for more details about available vulnerability methods). Using analytical-mechanic methods, the seismic input, that should also include possible site effect amplifications, can be directly represented by ground motion parameters (either peak or spectral) which can then be usefully combined with instrumental data available from in-situ monitoring of local amplification. On the other hand, the reliability of analytical vulnerability and damage estimation models is strongly influenced by the characteristics of the structures under examination, especially in regard to requested available information on

building characteristics. Moreover, these methodologies are well developed for reinforced concrete buildings but not sufficiently for masonry ones. Additionally, the application of analytical DEMs in urban areas is not easy because a large quantity of typological building information is required. For these reasons, especially on large territorial scale and particularly on historical urban centres, Damage Probability Matrices (DPMs) are generally used to estimate the building damage (Braga *et al.*, 1982; Dolce *et al.*, 2003). DPMs are an empirical damage estimation model (Calvi *et al.*, 2006) based on probabilistic distributions of expected damage for each EMS98 level (Grünthal, 1998) ranging from 0 (null damage) to 5 (total collapse). DPMs were set by Braga *et al.* (1982) by best fitting the post earthquake damage data associated with the 1980 Irpinia-Basilicata earthquake ($M_S=6.8$), observed for typical local building. Subsequently, DPMs have been updated by Dolce *et al.* (2003) to consider also the buildings with earthquake resistant design, realized or retrofitted after the 1980 earthquake. Then, this approach can be suitably applied to the building stock of Potenza because it was set up also considering the seismic performances of the local building types. However, when using this approach, it is rather difficult to take into account site effects estimated using modern methodologies and based on ground motion parameters. In fact, the seismic input required by DPMs has to be provided in terms of macroseismic intensity, possibly in EMS98 scale. Generally, the Medvedev (1962) method has been used to take into account site effects in DPM approach, (e.g. Dolce *et al.*, 2003). In Medvedev (1962) method the increase of macroseismic intensity due to soil amplification is roughly estimated on the base of the geological characteristics of the surface layers in the first 10 m depth. Particularly, the increments of macroseismic intensity are inversely proportional to the soil rigidity. In any case, this method does not account for an effective estimation of amplification obtained with instrumental measurements or in-situ analyses and modeling. Herein, in order to fill this gap, a new approach, based on the Housner intensity (Housner, 1952), has been developed. It combines the hazard at bedrock as defined by DSHA, the site effects information, and the Damage Probability Matrices, in order to define the most severe damage scenarios for the residential building stock at Potenza. Figure 1 shows the flowchart of the adopted methodology.

First, the seismic vulnerability of about 4200 buildings, present in the urban area of Potenza town, have been estimated. Subsequently, the PDFs of Housner intensity from DSHA have been defined for bedrock condition and subsequently convolved with the site transfer functions provided by Pacor & Mucciarelli (2007) in terms of Housner Intensity Ratio (HIR). Then, the PDFs for Housner intensity have been converted in PDFs for EMS98 intensity through a relationship defined in this study using data from past earthquakes. Finally, the PDFs for EMS98 intensity have been used as seismic input in DPMs in order to obtain the damage scenarios of the residential buildings under study. As a result, the distributions of urban building damage for each shaking scenario related to the causative considered faults have been proposed.

2. Deterministic seismic hazard analysis

A deterministic hazard study should firstly identify the reference earthquakes that will be expected to affect a particular area in the future and then apply a reliable seismological model to predict the ground motion. The ground motion estimated in this way for a given area of interest is called deterministic scenario (Reiter, 1990). As already said, in the present study “deterministic” refers only to the a priori choice of seismogenic sources and anelastic attenuation parameters. The damage at the site is then estimated considering the probability of different rupture scenarios as reported in the following sections.

2.1 Reference earthquakes

Potenza is a town in Southern Italy, located between the Apennines axial zone and the Apulia foreland, both corresponding to well-identified seismogenic zones (Figure 2). The Apulia Platform underlies the southern Apennines edifice and is the locus of the largest NW-SE striking, NW dipping normal faulting earthquakes that took place in this major seismogenic district (e.g., the 1857, Io=X-XI MCS, Val d'Agri earthquake; the 1980, M6.9, Irpinia earthquake, see Improta *et al.*, 2003). The large hypocentral depth (>15 km) of recent moderate events occurred in this region (i.e., the 1990-91, M5.8 and M5.1 Potenza earthquakes, and the 2002, M5.8 and M5.7 Molise earthquakes), however, suggests that they nucleated well below the Apulian platform (Azzara *et al.*, 1993; Chiarabba *et al.*, 2005). Tectonic studies on these events and other historical earthquakes in the area revealed a rather systematic pattern of EW striking right-lateral strike-slip faulting (Valensise *et al.*, 2004; Di Bucci *et al.*, 2006; Fracassi & Valensise, 2007). The area within 50 km distance from Potenza was affected by several destructive earthquakes in historical time (CPTI Working Group, 2004) and numerous seismogenic source are identified. The faults illustrated in Figure 2 are those that appear in DISS v. 3.0.2, a database of seismogenic sources for Italy and some surrounding countries (DISS Working Group, 2006; Basili *et al.*, 2008), with the exception of the F9 source. This fault has been hypothesized on the basis of detailed morphotectonic and geological investigations, several electrical resistivity tomographies and a palaeoseismological trench of the Scorciabuoi Fault (Caputo *et al.*, 2007). Table 1 lists the main geometric and focal parameters of the identified seismogenic sources.

2.2 Strategy for DSHA

The expected ground motions produced by the reference earthquakes at Potenza town are obtained through physics-based deterministic methods. They compute the ground motion at the surface through the convolution of the source-time function with the Green's functions (representation theorem, Aki & Richards, 2002). Deterministic simulation techniques are able to reproduce important effects related to the kinematic of the earthquake source, such as directivity, permanent displacement, long-period pulses, and effects related to the slip asperities distribution. Furthermore, the predicted ground motion can be expressed through different strong motion parameters, as peak and/or integral values. As said before, the ground motion variability is obtained varying the rupture kinematic parameters (slip velocity, rupture velocity, nucleation point, slip distribution). In this approach we assume that some large-scale parameters (e.g., fault geometry and orientation, seismic moment) can be considered, in average, constant in successive rupture episodes occurring on the same seismogenic fault but being unknown the details of a single rupture episode in the case, for instance, of a future event. The simulation of a large number of rupture models on a given fault will generate a large number of synthetics that can be statistically analyzed to infer the probability distributions (and then the associated statistical quantities) for the strong ground motion parameters of interest (Cultrera *et al.*, 2010). In the case study of Potenza, the ground motion estimations were first obtained by a simplified simulation method (level 1) for all the 9 seismogenic sources, in order to identify the faults able to likely produce the maximum expected shaking at the site, in terms of PGA, PGV and Housner intensity. Then, the reference earthquakes selected from the analyses performed at the level 1 were modeled with a full-wave simulation method (level 2), in order to calculate synthetics to be used for damage scenarios. The simulation approach used at the level 2 provides a more complete description of the ground motion with respect to that obtained at the level 1, and includes also suitable estimates of the low frequency ground motion (e.g., velocity and displacement time series) and engineering parameters strictly related to the duration of the signals (e.g., the Arias intensity). Ground motions at level 1 are simulated by the Deterministic Stochastic Method

(DSM; Pacor *et al.*, 2005) that introduces the finite-fault effects in the frame of the point source stochastic model proposed by Boore (2003). It has been applied in several studies of shaking scenarios for engineering applications (Ameri *et al.*, 2008; Emolo *et al.*, 2008; Ameri *et al.*, 2009). Due to its stochastic nature, DSM provides a reliable description of the high frequency ($f_z > 0.5\text{Hz}$) content and generates approximated synthetic accelerograms reproducing only the direct S wave-field, allowing a fast computation of synthetic seismograms in the frequency band of main engineering interest [0.5-10Hz]. The simulation technique Hybrid Integral-Composite method (HIC), recently proposed by Gallovič & Brokešová (2007), was adopted to compute shaking scenarios at the level 2, since it provides broadband synthetic seismograms. According to this technique, the rupture process at the seismic source is described in terms of slipping of elementary sub-sources, and combined with the discrete wave-number technique to obtain full wave-field Green functions for one-dimensional propagation medium. At low frequencies the source description is based on the representation theorem (integral approach, Aki & Richards, 2002), while at high frequency, the ground-motion synthesis is obtained summing the contributions from each individual sub-source treated as a point source (composite approach).

2.3 Bedrock scenarios at levels 1 and 2

As said in the previous section, the ground motions at levels 1 and level 2 have been computed with DSM and HIC, respectively. For the calculation of the Green's functions, a simplified 1-D crustal model valid for the area (Table 2; Amato & Selvaggi, 1993; Improta *et al.*, 2003) has been adopted. The frequency-dependent anelastic attenuation term, required by the DSM technique, has been described through the quality factor proposed by Rovelli *et al.* (1988) for Central and Southern Apennines and given by $Q(f)=100f$. Finally, the high frequency decay parameters has been set to $k_0=0.035s$, that is the value valid for rock sites (Margaris & Boore, 1998).

The different rupture models have been then obtained by varying the position of the nucleation point, the rupture velocity, and the final slip distribution. In particular, we used the k-squared slip model (Herrero & Bernard, 1994; Gallovič & Brokešová, 2004) to compute the final slip distribution on the fault. With DSM, the reference sources, whose geometry and focal parameters are listed in Table 1, have been modelled considering different rupture models for each fault, depending on the earthquake magnitude: 15 models have been considered for $M < 6.5$ events (obtained combining 5 rupture velocities by 1 slip model by 3 nucleation points) and 30 models for $M \geq 6.5$ earthquakes (5 rupture velocities by 2 slip models by 3 nucleation points). The nucleation points have been located in the lower half of the fault, close to the left and right edges and near the centre, in order to reproduce forward and backward directivity effects and bilateral rupture propagation at Potenza. In the DSM simulations, 2 slip distributions have been considered for each fault having magnitude $M \geq 6.5$ (F1, F3, F5, F8, F9): one is characterized by a random slip distribution and the other one having an asperity located close to Potenza. For the faults corresponding to earthquakes with $M < 6.5$ (F4, F6, F7) only a random slip distribution has been considered. The rupture velocities have been selected as a fraction of shear velocity V_s at hypocenter, between $0.7V_s$ and $0.9V_s$ in order to simulate both slow and fast rupture propagation along the fault. The F2 source has not been considered in the analysis due to its small dimension with respect to the F1 source. A statistical analysis has been performed on ground parameters predicted by different rupture scenarios on each fault in order to identify the sources producing the maximum shaking experienced at Potenza. The box plots in Figures 3 represent the statistical parameters inferred for peak ground acceleration PGA, velocity PGV, and Housner intensity at Potenza.

Each box encloses 50% of the data with the median value displayed as a thin line and the top and the bottom of the box mark the limits of $\pm 25\%$ of the population (see Figure 3 caption for more details). At Potenza, the median PGAs at level 1 range from 0.3 to 0.7 m/s^2 , with maximum values up to 2 m/s^2 while the median PGVs vary from 0.05 m/s and 0.12 m/s , with maximum values up to 4 m/s . The F6 and F7 faults produce PGA median values higher than those obtained from the other faults considered. In any case, however, the highest variability is found to be associated with the larger faults. In particular, the F8 source produces the highest peak values, due to the particular position of Potenza with respect to the fault plane, which makes the city prone to directivity effects. The PGV and I_H distributions show similar features: for both parameters, the median values associated with different faults are comparable each other and only the F3 and F8 sources generate slightly larger values. However, these two reference earthquakes produce the largest values and variability due to the particular source-to-site configuration. The computed values are also compared with the Italian Ground Motion Predictive Equation (GMPEs, Bindi *et al.*, 2009) for fault distances in the range 5 – 30 km, where most of the faults lie. Empirical PGVs fall, almost all, within the 25th and 75th percentile of the distributions associated with synthetics (Figure 3), with the exception of the F6 and F7 sources, whereas empirical PGAs slightly overestimate the DSM results. From the analysis of the top panels in the Figure 3, it is possible to infer that the maximum shaking scenarios at Potenza are produced by the F3, F7 and F8 faults and then we chose to consider just them to compute the ground motion at level 2. Simulations at level 2 are performed sampling more densely the kinematic parameters space. In particular, rupture scenarios considered several rupture velocity values, 6 slip distributions and a number of nucleation points larger than DSM scenarios. For instance, in the case of the F3 source, about 4000 rupture models have been simulated, densely sampling the nucleation point locations (i.e., considering 133 different hypocenters) and considering 5 rupture velocities. The simulation results are summarized in terms of PGA, PGV and I_H (Figure 3, bottom panels). The HIC simulations seems to provide larger shaking values than DSM: the median PGAs are in fairly good agreement with the empirical results, whereas PGVs overestimate the empirical estimates. However, this could be mainly due to the larger number of directive scenarios (rupture point very close the fault border, in the opposite direction with respect to the position of Potenza) used in the HIC modeling. Otherwise, the values provided by the two methods are comparable within their respective variability. For each fault, we plotted in Figure 4 the distribution of the predicted ground motion parameters (PGA, Housner intensities) at Potenza.

Due to its smaller dimension, F7 produces the lower ground motion variability. On the other hand, the F8 source generates the largest peak values in according with results obtained at the level 1 analysis. Looking at PGA and Housner intensity, these two parameters do not seem to follow the same distributions. In particular, in the case of F3 and F8 faults, the PGA follows approximately a log-normal distribution. On the other hand, the I_H distributions have different shapes that seem to be bi-modal for F3 and F8. Each ground motion parameter represents different characteristics of the seismogram and accounts for different frequency content of the seismic radiation spectrum. In particular, the I_H is mainly controlled by the coherent low-to-intermediate frequency ground motion and depends on the large scale properties of source and propagation medium. On the other side, PGA is mainly related to the high-frequency content of the ground motion.

Several statistical quantities can be inferred from the parameters distributions to be used for damage analysis, such as, the mean value and the associated standard deviation, the median, the 75th and 84th percentiles, the mode, and minimum and maximum values. In any case, in this work the PDFs for Housner intensity, for each fault, have been directly used as seismic input for building damage scenarios, as discussed before. On the basis of the small size of the

urban area (see Figure 5), the PDFs estimate at bedrock are held constant over the whole area and subsequently they are modified only for the contamination introduced by site effect as reported in the next section.

2.4 Convolution of PDFs at bedrock with site effects

Soil amplification surveys were carried out, in the framework of DPC-INGV S3 project (Pacor & Mucciarelli, 2007) at 14 sites within the urban area of Potenza. For the analysis both the reference and non-reference site techniques were used. To evaluate the site response, a temporary network (since October 2004 to May 2005) was installed in the town to record both local and regional seismicity (~250 events). Furthermore, the Housner intensities and the mean ratios (Housner Intensity Ratio, HIR) with respect the reference site, for each recording corresponding to local earthquakes (~25 events) were computed. In order to extend the detailed site response obtained using earthquake time series, a dense set of single station noise measurements were performed (~230 points), thus computing the Horizontal-to-Vertical Spectral Ratios (HVSRS). The measurements were distributed over the city area, sampling different kind of lithologies and slopes. Particularly, using a correlation technique that combines the Pearson Coefficient and degree of fit, the 230 HVSRS curves (single station measurements) were correlated to the HVSRS functions at the 14 sites where the long-term monitoring was performed, each of them being characterized by one HIR value. The HIR correction coefficients were extended to the 230 locations where they were averaged over districts, within the city, in which the building stock was surveyed. This procedure allowed to provide a microzonation map of the urban area of Potenza with site effects correction coefficient (HIR) between 1 (no amplification) and 1.7 (higher value of the Housner Intensity amplification). Figure 5 shows the seismic microzonation of the urban area of Potenza. More details about the seismic microzonation of Potenza can be found in Pacor & Mucciarelli (2007).

In the framework of this paper, each PDF for Housner intensity evaluated from synthetic seismograms simulated at the bedrock has been multiplied by the value of HIR relevant to any considered district. As a result, in each district of Potenza urban area a PDF in terms of Housner intensity has been provided for each fault shaking scenario, also including the studies of site effect amplification.

3. Probability Density Functions in EMS98 intensity

As already described, the Damage Probability Matrices (DPMs) approach (Braga *et al.*, 1982; Dolce *et al.*, 2003) has been selected as damage estimation model. For this reason, the Housner Probability Density Functions (H-PDFs) obtained by the Deterministic Seismic Hazard Analyses (DSHAs) need to be given in terms of the EMS98 intensity (I_{EMS}) (Grünthal, 1998). To this end, many studies (e.g., Margottini *et al.*, 1992; Decanini *et al.*, 2002; Faccioli and Cauzzi, 2006) have been devoted to obtaining similar relationships between macroseismic intensity (usually in MCS scale) and ground motion parameters (generally PGA and PGV). Herein, a relationship between I_H and I_{EMS} has been derived. Through this relationship, the H-PDFs provided by the ground motion simulations have been converted in PDFs for I_{EMS} , either including or neglecting the site effects.

3.1 Housner Intensity versus EMS98 Intensity

In the present section the proposed relationship between Housner and EMS98 intensities is presented and discussed. Housner (1952) was the first at searching for a similar relation

between the Mercalli Modified Intensity (MMI) and the values of I_H computed for some time series from some California earthquakes recorded in the same urban areas. In the present study, a sample of about sixty earthquake recordings (see Appendix) have been selected from the Italian Accelerometric Archive (Working Group ITACA, 2008), that mostly contains Italian earthquakes having a known macroseismic local intensity estimated in areas close to the accelerometric station (Margottini *et al.*, 1992). Moreover, in order to enrich the data set, data from the 1999 Izmit earthquake (M7.6) (available from the European Strong Motion Database, Ambraseys *et al.*, 2004), as well as from the 1997 Umbria-Marche (M5.6) and the 2002 Palermo (M5.9) earthquakes (available from ITACA database), have been added. To perform the regression between I_H and I_{EMS} , seismograms recorded in the same local area where macroseismic intensity data are available in the EMS98 scale, are required. Unfortunately, for the Italian territory no data with $I_{EMS} \geq VIII$ are available joint with ground motion time series. Concerning the macroseismic intensity scale, in some studies (e.g., Codermatz *et al.*, 2003) it is concluded that a substantial equality exists between Mercalli-Cancani-Sieberg scale (MCS; Sieberg, 1930) and the European definition of macroseismic intensities (MSK76, EMS92 and EMS98). The MCS scale is used mainly to estimate intensities for historical earthquakes. However, when a re-estimation of the intensities was carried out (e.g., in the case of the 1976, M6.5 Friuli earthquake) results show that, for intensities larger than VII, the EMS and MCS scales may differ by one degree or more (Molin, 1995). For this reason, in this paper a more restrictive approach is followed, adopting only the equality between EMS98 (Grünthal, 1998) scale with MSK-76 (Medvedev, 1977) and EMS92 (Grünthal, 1993) scales. In fact, only these scales take into consideration a precise definition of building vulnerability and observed damage distributions in assigning the intensity value. Then, for each available seismogram, the acceleration time history has been converted in pseudovelocity spectrum $PVS(T, \xi)$, where T is the period of a system characterized by a single degree of freedom (SDOF) and ξ is the fraction of critical damping. Subsequently, the I_H is computed as the area under the pseudovelocity spectrum in the range of period between 0.2 and 2 seconds (Equation 1):

$$I_H = \int_{0.2}^2 PVS(T, \xi) dT \quad (1)$$

The value of 5% has been adopted for the fraction of critical damping in computing the $PVS(T, \xi)$. It is worth noting that, while I_H is usually computed in the period range between 0.1 and 2.5 s, in the present work a period range between 0.2 and 2 seconds has been used because such a range is considered to provide values better correlated with the damage potential of ground motion when dealing with ordinary building structures. Moreover, our choice agrees with the choice adopted in the seismic reclassification of the national Italian territory proposed by GNDT Working Group (1999) and it is also coherent with the site effects analyses (Pacor & Mucciarelli, 2007) where I_H has been computed in the period range of 0.2-2 s for avoiding the bias due to low signal-to-noise ratios for period values outside this range in the analysis of local earthquake spectra. Figure 6 reports the values of EMS intensity as a function of the natural logarithm of the Housner intensity values (maximum of the two horizontal components). As it could be expected, in the range of intensities up to V-VI EMS a little variation of I_H can be found. In fact, at these lower intensities damage is substantially absent, and intensity degrees are assigned prevalingly on the basis of effects on people and objects. For degrees higher than VI EMS, damage distribution and severity (therefore I_H values) becomes the key element to assign intensity. To obtain an unbiased estimate, two separate regressions have been computed, starting from opposite ends of I_H distribution, and calculating corresponding correlation coefficients. The distributions of the correlation coefficient with respect to I_H shows a changing point which is common for both right wise and left wise calculations at 0.18 m. Thus, as a result of the observation of two different trends in the selected data, a bilinear regression has been proposed.

Specifically, for values of Housner intensity greater than 0.18 m (-1.7 m in terms of natural logarithm) a linear tendency with a significant correlation coefficient ($R=0.88$) is observed. On the other hand, for values of Housner intensity smaller than 0.18 m, which are coupled to medium-to-low values of EMS intensities, a different behaviour with a poor correlation ($R=0.36$) is found. This is not surprising because, from one side, I_H is well correlated to the damage potential of seismic events while, on the other hand, low macroseismic intensity values mean negligible damage on buildings, as in the case of I_H values lower than 0.18 m that corresponds to V-VI EMS (Figure 6). Therefore, to convert the Housner into the respective EMS intensities, the following expressions (2) and (3), respectively for values of I_H greater and lower than 0.18 m (-1.7 m in terms of natural logarithm), are proposed:

$$I_{EMS} = 1.41 \cdot \log_e(I_H) + 7.98 \quad I_H \geq 0.18m \quad (2)$$

$$I_{EMS} = 0.27 \cdot \log_e(I_H) + 6.02 \quad I_H < 0.18m \quad (3)$$

Equations (2) and (3) provide values for the macroseismic intensity in a continuous form, thus a conversion into the discrete degrees of EMS intensity scale is required. In this work, we chose to approximate the macroseismic intensity derived from the relationships (2) and (3) to the nearest integer value, for intensities ranging between V to IX EMS, as shown in Figure 7.

3.2 PDFs for the EMS98 intensity

Starting from the PDF distributions for Housner intensity, obtained by the DSHA approach, and after having modified them including the site amplification coefficients, it is possible to retrieve the relevant PDFs for the EMS98 intensity by means of the equations (2) and (3) that, as explained before, have to be used for values of I_H greater and smaller than 0.18 m, respectively. Preliminarily, let us discuss the results obtained without including the site effects. This case is shown in the Figure 8 where we present the PDFs for EMS98 intensity, in the range from V to IX EMS, for each shaking scenario.

The highest seismic severity is associated with the F8 source which is characterized by probabilities of 34% and 10% to produce I_{EMS} values equal to VIII and IX, respectively. The F3 source provides intermediate values, with 37%, 27% and 5% of probability to obtain I_{EMS} values equal to VII, VIII and IX, respectively. The shaking scenario corresponding to the F7 fault presents the lower values of macroseismic intensity that range between V (79% of probability) and VI (21%) EMS.

The next step is to perform a similar analysis for the PDFs that include the site effects. Even if we have already explained before the procedure we adopted to this end, let us recall here that any I_H value returned from the synthetic seismograms generated by the DSHA approach for each source, has been firstly multiplied by the local HIR value. Subsequently, the relationship I_{EMS} vs I_H (Equations 2 and 3) has been used to obtain the associated EMS98 intensity. The results obtained in this case are shown in the Figure 9, where the PDFs for the EMS98 intensity are reported for the different amplification zones. For cleanness of draw, let us also recall here that the HIR values have been summarized in three homogeneous amplification areas: no or low (HIR between 1.0-1.2, in the graph HIR=1), medium (HIR between 1.3-1.5, in the graph HIR=1.4) and high (HIR between 1.6-1.7, in the graph HIR=1.7).

The highest seismic severity is associated with the F8 source that shows PDF values of 33%, 26% and 6% respectively for VIII, IX and X EMS when HIR=1.7, respect to 34%, 10% and 0% neglecting site effects. For F3 source, the values of PDF increase to 20% and 38% respectively for VIII and IX EMS when HIR=1.7 respect to the values of 5% and 27% without including site effects. The shaking scenario corresponding to the F7 fault confirms the lower values of macroseismic intensity that range between V (47% of probability) and VI (50%) EMS when HIR=1.7. For this fault considering HIR=1.7 a value of 3% is shown also for VII EMS.

4. Building stock analysis and vulnerability assessment

After the 1990 Basilicata earthquake (Azzara *et al.*, 1993) the Potenza building stock (about 12000 units) was completely surveyed using the 1st level GNDT90 inspection form for damage and vulnerability evaluation (GNDT Working Group, 1990). As well as damage data, geometrical and quantitative characteristics of all the buildings were also collected, including height, plan and elevation configurations, age, type of vertical and horizontal structure, type of foundation and roof, possible retrofitting, state of preservation, etc. In 1999, the building inventory was firstly updated to include the buildings built after 1990, which had reinforced concrete (RC) structure (Dolce *et al.*, 2003). A second updating aimed at correcting and integrating building data was recently (2007) carried out by the authors in some urban areas of the town.

The building stock of the entire Potenza territory has already been analysed in previous seismic risk studies (Dolce *et al.*, 2003; 2006). In this paper only the urban area of the town, where about 4200 private buildings (about $11 \cdot 10^6$ m³ in volume) are present, has been studied. Table 3 shows the distribution, in terms of number and volume, of the more widespread building types. It should be noted that a different composition of the building stock emerges when the number or the volume of the buildings are considered. In terms of numbers, the sample is mostly made up of masonry (56%) rather than RC structures (42%). On the contrary, in terms of volume there is a significant prevalence of RC buildings (76%) with respect to masonry structures (22%). The other structural types (special type, steel, wooden, etc.) are very rare (2% both in terms of number and volume).

Table 4 shows the distribution in terms of age of masonry and RC buildings. Old masonry buildings, built before the '70s, prevail (about 32% in number and 13% in volume) over the new ones (14% in number and 3% in volume). RC buildings were mostly built after 1970 (24% in number and 41% in volume). After the 1980 Irpinia-Basilicata earthquake the area of Potenza town was classified as a seismic zone for the first time, and as a consequence, from then on new buildings were designed using seismic criteria. Furthermore, 10% of masonry buildings (6% of volume) have been seismically retrofitted after 1980, while the percentage of retrofit for RC buildings is currently 5% in number (13% in volume).

Utilizing a DPM approach as discussed in Dolce *et al.* (2003), a vulnerability class was assigned to each building starting from its most important structural characteristics, that is age of construction and/or of retrofitting, horizontal and vertical structural type. The vulnerability classes A, B, C, and D considered in the EMS-98 scale (Grünthal, 1998) relevant to high, medium, medium-low and low vulnerability, respectively, were used. The choices adopted herein in assigning a vulnerability class to each building are reported in Table 5. A low vulnerability (class D) has been proposed for the structures built or retrofitted according to the seismic classification after 1980 (Dolce *et al.*, 2003).

In Table 6 the number of buildings for each set with the same vulnerability class is reported. Table 7 summarizes the vulnerability distributions in terms of building number and volume.

The building stock of Potenza town has a prevalence of low to medium vulnerability (classes D and C). Specifically, 34% of building stock belongs to class D (41% in terms of volume), and 39% belongs to class C (49% in terms of volume). Lower percentages of buildings have either high vulnerability (class A, 13% in terms of number and 5% in volume) or medium vulnerability (class B, 14% in terms of number and 5% in volume).

Regarding to site effects, Figure 10 shows, for each vulnerability class, the number of buildings located in zones affected by different local amplification. Only about 15% of the considered 4200 buildings are located in areas characterized by large amplifications (HIR=1.6-1.7). In any case, even though most of the buildings (about 80%) are located in a medium amplification zone (HIR=1.3-1.4), they have generally low vulnerability (classes D and C).

5. Damage scenario

The preparation of the damage scenario is the comprehensive final step that, by combining building vulnerability and earthquake shaking, and possibly including also the site effects, returns the estimation of the building damage and, as a consequence, of the relative losses (e.g. human casualties, economic losses) whose estimation is fundamental in seismic risk prevention and management. As already been said, the damage distribution in the building stock caused by the above described three shaking scenarios (sources F3, F7 and F8) has been evaluated using the DPM approach. For each shaking scenario, the number of buildings for each district of Potenza town suffering a certain damage level L_d has been computed as follows:

$$N(L_d) = \sum_i \sum_j P_i N_j DPM(i, j, L_d) \quad (4)$$

where L_d are the damage levels, as provided in the EMS98, ranging between 0 and 5 ($L_d=0$ means total absence of damage, while $L_d=5$ means total destruction of the building), P_i is the probability of having an EMS98 intensity i (between V to X EMS, see Figure 9), and N_j is the number of buildings for each vulnerability class j (A, B, C and D). $DPM(i, j, L_d) = P[L_d/j, i]$ is the probability of obtaining a damage level L_d given a macroseismic intensity i and a vulnerability class j . The values of $DPM(i, j, L_d)$ adopted in this paper are reported in Dolce *et al.* (2003) for the intensity degrees between VI and X EMS, while, as for the V degree, damage level frequencies have been derived by accounting for the suggestions reported in the EMS98. Generally, shaking scenarios are provided in a deterministic form, e.g. by referring to the maximum credible or the most probable earthquake. Therefore, in applying the DPM approach, just one macroseismic intensity value is used to prepare building damage scenarios. On the contrary, in the present study, a probabilistic distribution for the macroseismic intensity has been used. This is possible because, using the relationship that provides I_{EMS} as a function of I_H (Equations 2 and 3), the results of DSHA, available in terms of seismic instrumental parameters, specifically Housner intensity, can be converted into probabilistic distributions for the related macroseismic intensity. In Figure 11 and Table 8, for each damage level the number of buildings affected by the three earthquake scenarios F8, F7 and F3, with (w SE) and without (w/o SE) site effects on all the urban area of town, is shown.

On about 4200 investigated buildings, the percentages of heavily damaged and collapsed buildings (damage level ≥ 4) is equal to 8% and 6%, respectively, for the sources F8 and F3

without including site effects. These values increase up to 12% and 10% taking into account site effects. The influence of site effects on the damage distribution is remarkable: when site effects are considered, the amount of heavily damaged and collapsed buildings increases in percentage by about 50% and 60%, respectively, for the scenarios associated to the F8 and F3 sources. For the source F7, the number of heavily damaged buildings is practically null, even if we include the site effects. In Table 9, for each damage level, the total volume of buildings affected by the three earthquake scenarios F8, F7 and F3 (with and without site effects), is shown. The damage distributions in terms of building volume confirm the results already obtained in terms of building numbers.

To obtain a global estimation of building damage due to the selected shaking scenarios the mean damage index DI_{med} (Dolce *et al.*, 2003) has been calculated through the expression:

$$DI_{med} = \sum_i^n \frac{L_{di} f_i}{n} \quad (5)$$

where L_{di} is the damage level, varying between the first and fifth levels of EMS-98 damage scale, and f_i is the relevant frequency of occurrence. The summation does not include the null damage level, therefore DI_{med} varies between 0 and 1, where $DI_{med} = 0$ means total absence of damage and $DI_{med} = 1$ means total destruction of the building stock. DI_{med} is not an exhaustive representation of the damage distribution but it provides a synthetic estimation of the effects due to different seismic inputs as well as an easy way to compare them. Table 10 reports the DI_{med} values for each building damage scenario, with and without site effects.

The highest values of DI_{med} are found for the F8 source, where values equal to 0.45 and 0.42 are computed considering and neglecting soil amplification, respectively. As could be expected, lower values of DI_{med} are found for the F7 source, with a small variation when site effects are included or not. These results show that significant levels of global damage can be predicted, on average, for the urban area of Potenza considering F8 and F3 sources. On the contrary, F7 source returns lower damage due to the low severity of wave field, as discussed in the above paragraphs. The results have been subject to further analysis to obtain an estimation of expected losses in terms of unusable buildings. For this purpose, the number of unusable buildings has been computed using the procedure, widely adopted in Italy, developed by Lucantoni *et al.* (2001) on the basis of surveyed data after past earthquakes. According to such a procedure, all the buildings with damage level $L_d \geq 4$ and a portion (40%) of the buildings with $L_d = 3$ are considered unusable. In Table 11 the percentages of unusable buildings for each shaking scenario, considering or not considering site effects, are reported.

In terms of building numbers, the F8 damage scenario returns an estimation of 500 and 700 unusable buildings when neglecting or considering soil amplification, respectively. Considering the source F7, this number decreases drastically to values lower than 80. Finally, also the source F3 returns large values of unusable buildings (590 and 420 with and without site effects, respectively). In terms of building volume, the percentages of unusable buildings are remarkably lower as a consequence of the higher average volume and lower vulnerability of buildings having Reinforced Concrete structure.

6. Final remarks and future developments

Building damage scenarios have been calculated for the urban area of Potenza combining a deterministic choice of seismogenic sources with probabilistic estimates of earthquake shaking at bedrock, site effects and building damage. The use of simulation techniques allows to better take into account the complex nature of ground shaking, at a given site, and to compute synthetic seismograms. The simulated accelerograms can be analysed in order to estimate ground motion parameters of engineering interest which can be used as seismic input for building damage scenarios. In particular, a preliminary earthquake modeling allowed us to identify the three sources (among nine) potentially most hazardous for Potenza. For each fault, a large number of possible rupture processes at the source have been considered and, for each of them, the synthetic seismograms at Potenza for bedrock conditions have been simulated. Then, a soil amplification map, drawn in the framework of DPC-INGV S3 project using Housner Intensity Ratios (HIR), has been combined with the results of shaking ground motion at bedrock. As a results, probability density functions (PDFs) for Housner intensity including the site effect amplifications (H-PDFs) have been defined at the site of Potenza. After that, a relationship between EMS98 and Housner intensities has been developed, on the basis of strong motion recordings and macroseismic data catalogues. Using this relationship, the H-PDFs provided by DSHA and convolved with site effects, have been converted in EMS98 intensity PDFs which have been used as input of the Damage Probability Matrices (DPMs). Differently from the procedures typically adopted in the preparation of damage scenarios, that enter only one value of macroseismic intensity in the DPMs, in this work a probabilistic distribution of macroseismic intensity has been used as input. As a result, a probabilistic approach has been adopted, involving complex source models, site effects estimation and damage estimation model. The computed damage scenarios emphasise a generally low vulnerability in the urban centre of Potenza town and, then, a limited number of damaged buildings for the lower intensity, and of partially or totally collapsed building, for the higher intensity earthquakes. Particularly, with respect to the F3-Irpinia and F7-Potenza sources, the F8-Andretta-Filiano fault returns the highest damage. Moreover, the influence of site effects on the damage distribution is quite significant. Considering the F8 source, the scenario that includes the site effects provides a number of partially or totally collapsed buildings of about the 50% higher than the value computed without site effects. Although many questions are still to be addressed and resolved, the proposed approach aims at showing how a multidisciplinary methodology, based on different competences and points of view, but having the same goal, is suitable for define the expected building damage scenarios at urban scale.

Acknowledgements

The work presented in this paper was partially funded by the S3 R Research Project in the framework of the 2006-2006 agreement between the Italian Civil Protection and the National Institute of Geophysics and Volcanology. The authors are grateful to Roberto Basili who provided us the faults characteristics used in study. Some stimulating discussions with Dr. S. Parolai and Dr. A. Strollo of GeoForschungsZentrum of Potsdam are gratefully acknowledged.

Appendix: Macroseismic and Housner Intensity data

(I_H value has been computed in the period range 0.2-2 s with 5% damping)

Data	Epicentral Area	Station	Housner Intensity [m]	Local Intensity [EMS]
1980/11/23	Irpinia	Arienzo	0.08	6 ^(*)
		Bisaccia	0.52	6 ^(*)
		Bovino	0.11	5 ^(*)
		Brienza	0.34	6.5 ^(*)
		Calitri	0.93	7.5 ^(*)
		Mercato San Severino	0.37	6.5 ^(*)
		Rionero in Vulture	0.45	7 ^(*)
		Sturno	1.13	7.5 ^(*)
		Torre del Greco	0.21	5.5 ^(*)
		Tricarico	0.19	5.5 ^(*)
		Bagnoli Irpino	0.90	7 ^(*)
		Auletta	0.18	6 ^(*)
		Benevento	0.26	6 ^(*)
1983/11/09	Parma	Fornovo di T.	0.04	6 ^(*)
1984/04/29	Gubbio	Pietralunga	0.18	6 ^(*)
		Umbertide	0.02	6 ^(*)
		Peglio	0.04	5 ^(*)
		Città di Castello	0.13	5 ^(*)
		Cagli	0.01	5 ^(*)
		Nocera Umbra	0.07	6 ^(*)
1984/05/07	Val Comino	Atina	0.13	7 ^(*)
		Pontecorvo	0.13	5 ^(*)
		Roccamonfina	0.13	6 ^(*)
		Ortucchio	0.09	5 ^(*)
		Barisciano	0.01	4.5 ^(*)
		Castelnuovo	0.06	5 ^(*)
		Lama dei pel.	0.12	6 ^(*)
		Scafa	0.22	6 ^(*)
		Poggio Picenze	0.02	5 ^(*)
Ripa Fagn.	0.03	5 ^(*)		
1984/05/11	Val Comino	V.Barrea	0.22	6 ^(*)
		Atina	0.03	6 ^(*)
		Lama dei pel.	0.03	5.5 ^(*)
		Scafa	0.05	5 ^(*)
1985/01/23	Garfagnana	Vagli Paese	0.02	4 ^(*)
		Sestola	0.01	5 ^(*)
		Barga	0.03	5 ^(*)
1985/05/20	L'Aquila	Barisciano	0.05	5 ^(*)
		Castelnuovo	0.01	5 ^(*)
		Poggio Pic.	0.03	6 ^(*)
		S. Dometrio V.	0.01	4 ^(*)
1987/04/24	Reggio Emilia	Sorbolo	0.005	5 ^(*)
		Novellara	0.038	5 ^(*)
1987/05/02	Reggio Emilia	Sorbolo	0.01	5 ^(*)
		Novellara	0.13	5 ^(*)
1997/09/26	Umbria-Marche	Nocera-Umbra	0.70	7 ^(**)
		Colfiorito	0.64	7.5 ^(**)
1998/09/09	Basilicata	Grumento Nova	0.14	4 ^(***)
		Lauria Gallo	0.23	6 ^(***)
		Lauria	0.29	6 ^(***)
		Scalea	0.19	5 ^(***)
		Viggianello	0.13	5.5 ^(***)
1999/08/17	Izmit, Turkey	Duzce	1.72	9 ^(****)
		Gebze	0.54	8 ^(****)
		Yarimaca	1.36	9 ^(****)
		Izmit	0.75	9 ^(****)
2002/09/06	Palermo	Castel di Iudica	0.02	4 ^(****)
		Caltagirone	0.02	4 ^(****)
		Patti	0.04	4.5 ^(****)

(*) Margottini *et al.*, 1992; (**) Stucchi *et al.*, 1998 (http://emidius.mi.ingv.it/GNDT/T19970926_eng/); (***) Galli *et al.*, 2001; (****) Camassi & Mucciarelli, 2002; (*****) Azzaro *et al.*, 2004.

References

- Amato A. & Selvaggi G., 1993. *Aftershock location and P-velocity structure in the epicentral region of the 1980 Irpinia earthquake*. *Annals of Geophysics*. 36, 3– 15.
- Ameri G., Akinci A., Cocco M., Cultrera G., Franceschina G., Pacor F., Pessina V., Lombardi A. M., 2007. *Ground motion scenario for selected cities (pp 41-58)*. In: *Technical dissemination N. 8 SP11 - Prediction of ground motion and loss scenarios for selected infrastructure systems in European Urban Environment* (Eds: Faccioli E.) IUSS Press, ISBN 978-88-6198-012-9, pp. 210.
- Ameri G., Pacor F., Cultrera G., Franceschina G., 2008. *Deterministic Ground-Motion Scenarios for Engineering Applications: The Case of Thessaloniki, Greece*. *Bulletin of Seismological Society of America*, 98, 3, 1289–1303.
- Aki K. and P.G. Richards, (2002). *Quantitative Seismology: Theory and Methods*, second edition. University Science Books.
- Ambraseys N., 1974. *Historical seismicity of north-central Iran*. *Geological Survey Iran* 29, 47– 96.
- Ambraseys N., Smit P., Douglas J., Margaris B., Sigbjorns-son R., Olafsson S., Suhadolc P., Costa G., 2004. *European Strong-Motion Database Volume 2, European Commission, Research-Directorate General, Environment and Climate Programme*. Available at web site <http://www.isesd.cv.ic.ac.uk/ESD/>
- Arias, A., 1970. *A Measure of Earthquake Intensity*. In *Seismic Design for Nuclear Power Plants*. R. J. Hansen, Ed . MIT Press, 438 – 483.
- Azzara R., Basili A., Beranzoli L., Chiarabba C., Di Giovanbattista R., Selvaggi G., 1993. *The Seismic Sequence of Potenza*. *Annals of Geophysics*, 36(1), 237–243.
- Azzaro R., Barbano M.S., Camassi R., D’Amico S., Mostaccio A., Piangiamore G. & Scarfi L. 2004. *The earthquake of 6 September 2002 and the seismic history of Palermo (Northern Sicily, Italy): Implications for the seismic hazard assessment of the city*. *Journal of Seismology* 8, 525–543.
- Basili R., Valensise G., Vannoli P., Burrato P., Fracassi U., Mariano S., Tiberti M.M., Boschi E., 2008. *The Database of Individual Seismogenic Sources (DISS), version 3: summarizing 20 years of research on Italy’s earthquake geology*. *Tectonophysics*, 453, 20-43.
- Bazzurro P. and C. A. Cornell (1999). *Disaggregation of seismic hazard* *Bulletin of the Seismological Society of America*, 89, 2, 501-520
- Bindi D., Luzi L., Massa M., Pacor F., 2009. *Horizontal and vertical ground motion prediction equations derived from the Italian Accelerometric Archive (ITACA)*. *Bulletin of Earthquake Engineering*. DOI 10.1007/s10518-009-9130-9.
- Bolt B.A. & Abrahamson N.A., 1982. *New attenuation relations for peak expected accelerations of strong ground motion*. *Bulletin of the Seismological Society of America*, Vol. 72, pp. 2307-2321.
- Bommer, J.J. (2002). *Deterministic vs. probabilistic seismic hazard assessment: an exaggerated and obstructive dichotomy*. *Journal of Earthquake Engineering* 6 (Special Issue 1), 43-73.
- Boore D.M., 2003. *Simulation of ground motion using the stochastic method*. *Pure Appl. Geophys.* 160, pp. 635-676.
- Braga F., Dolce M., Liberatore D., 1982. *A statistical Study on Damaged Buildings and Ensuing Review of the MSK-76 Scale*. 8th ECEE, Atene.
- Calvi G.M. & Pinho R., 2004. *LESSLOSS - A European Integrated Project on Risk Mitigation for Earthquakes and Landslides, Report 2004/02*. European School for Advanced Studies in Reduction of Seismic Risk (ROSE School), IUSS Press, Pavia, Italy.

- Calvi G.M., Pinho R., Magenes G., Bommer J.J., Restrepo-Vélez L.F., Crowley H., 2006. *Development of seismic vulnerability assessment methodologies over the past 30 years*. ISET Journal of Earthquake Technology, Paper o. 472, Vol. 43, No. 3, September 2006, pp. 75-104.
- Caputo R., Salviulo L., Piscitelli S. and Coperte A., 2007. *Late Quaternary activity along the Scorciabuoi Fault (Southern Italy) as inferred from electrical resistivity tomographies*. Annals of Geophysics, vol. 50, n. 2.
- Chapman M. C. (1995) A probabilistic approach to ground-motion selection for engineering design *Bulletin of the Seismological Society of America*; 85; 3; 937-942
- Chiarabba C., De Gori P., Chiaraluce L. and 21 others, 2005. *Mainshocks and aftershocks of the 2002 Molise seismic sequence, southern Italy*. Journal of Seismology, 9, 487-494.
- Codermatz R., Nicolich R., Slejko D., 2003. *Seismic risk assessments and GIS technology: applications to infrastructures in the Friuli–Venezia Giulia region (NE Italy)*. Earthquake Engineering and Structural Dynamics. 32:1677–1690 (DOI: 10.1002/eqe.294)
- Convertito V., Emolo A. and A. Zollo, 2006. *Seismic-Hazard Assessment for a Characteristic Earthquake Scenario: An Integrated Probabilistic–Deterministic Method*. Bulletin of Seismological Society of America, Vol. 96, No. 2, pp. 377–391, April 2006, doi: 10.1785/0120050024.
- Cornell, C.A. (1968). Engineering seismic risk analysis, *Bull. Seism. Soc. Am.*, 58, 1583-1606.
- CPTI Working Group, 2004. *Catalogo Parametrico dei Terremoti Italiani, version 2004 (CPTI04)*. INGV, Milan. Available from <http://emidius.mi.ingv.it/CPTI/>.
- Cultrera G., Cirella A., Spagnuolo E., Herrero, A; Tinti E. and F. Pacor (2010). Variability of kinematic source parameters and its implication on the choice of the design scenario, accepted on Bulletin of Seismological Society of America
- Decanini L., Mollaioli F., Oliveto G., 2002. *Structural and seismological implications of the 1997 seismic sequence in Umbria and Marche, Italy*. In Innovative Approaches to Earthquake Engineering, G. Oliveto (editor), Southampton, WIT Press, 229-323.
- Di Bucci D., Ravaglia A., Seno S., Toscani G., Fracassi U., Valensise G., 2006. *Seismotectonics of the Southern Apennines and Adriatic foreland: insights on active regional E-W shear zones from analogue modelling*. Tectonics, 25, TC4015, doi: 10.1029/2005TC001898.
- DISS Working Group, 2006. *Database of Individual Seismogenic Sources (DISS), Version 3.0.2: A compilation of potential sources for earthquakes larger than M 5.5 in Italy and surrounding areas*. <http://www.ingv.it/DISS/>, © INGV 2005, 2006 - Istituto Nazionale di Geofisica e Vulcanologia - All rights reserved.
- Dolce M., Masi A., Marino M., 2002. *EAAE-ESC Task Group 3 – Seismic risk and earthquake scenarios - Report of the activities in the frame of the ENSeRVES Project*, Proc. of 12th European Conference on Earthquake Engineering, September 2002, London.
- Dolce M., Masi A., Marino M., Vona M., 2003. *Earthquake damage scenarios of Potenza town (Southern Italy) including site effects*. Bulletin of Earthquake Engineering, Vol. 1, N. 1, pp. 115-140.
- Dolce M., Kappos A.J., Masi A., Penelis G., Vona M., 2006. *Vulnerability assessment and earthquake scenarios of the building stock of Potenza (Southern Italy) using the Italian and Greek methodologies*. Engineering Structures, Vol. 28, 357-371.
- Emolo A., Zollo A., 2001, Accelerometric radiation simulation for the September 26, 1997, Umbria-Marche (Central Italy) main shocks, Annals of Geophysics, 44, 605-617.
- Emolo A., Cultrera G. Franceschina G., Pacor F., Convertito V. Cocco M., Zollo A., 2008, *Ground motion scenarios for the 1997 Colfiorito, central Italy, earthquake*, Annals of Geophysics, 51, 509-525.
- ENSeRVES, 2000. *European Network on Seismic Risk, Vulnerability and Earthquake Scenarios*. Proceedings International Workshop on Seismic Risk and Earthquake Scenarios of Potenza, University of Basilicata, Italy.

- Faccioli E., Pessina V., Calvi G.M., Borzi B., 1999. *A study on damage scenario for residential buildings in Catania city*. Journal of Seismology, 3(3), 327-343.
- Faccioli E. & Cauzzi C., 2006. *Macroseismic intensities for seismic scenarios, estimated from instrumentally based correlations*. European Conference on Earthquake Engineering and Seismology, Geneva, Switzerland, 3-8 September 2006.
- Fracassi U. & Valensise G., 2007. *Unveiling the sources of the catastrophic 1456 multiple earthquake: Hints to an unexplored tectonic mechanism in Southern Italy*. Bulletin of Seismological Society of America, 97, 3, 725-748, doi: 10.1785/0120050250.
- Galli P., Molin D., Camassi R., Castelli V., (2001). *Il terremoto del 9 settembre 1998 nel quadro della sismicità storica del confine calabro-lucano. Possibili implicazioni sismotettoniche*. Il Quaternario - Italian Journal of Quaternary Sciences, 14, 31-40.
- Gallovic F. & Brokešová J., 2004. *On strong ground motion synthesis with k-2 slip distributions*. Journal of Seismology 8, 211-224.
- Gallovič, F. & Brokešová J., 2007. *Hybrid k-squared Source Model for Strong Ground Motion Simulations: Introduction*. Phys. Earth Planet. Interiors, 160, 34-50.
- GNDT Working Group, 1990. *Evento sismico 05/05/1990. Scheda per il rilevamento dei danni. Istruzioni per la compilazione*. Presidenza del Consiglio dei Ministri – Ufficio del Ministro per il Coordinamento della Protezione Civile. Roma.
- GNDT Working Group, 1999. *Proposta di riclassificazione sismica del territorio nazionale*. Ingegneria Sismica, Anno XVI N.1, gennaio-aprile.
- Grünthal, G. (editor), 1993. *European Macroseismic Scale 1992 (EMS-92)*. European Seismological Commission, sub commission on Engineering Seismology, working Group Macroseismic Scales. Conseil de l'Europe, Cahiers du Centre Européen de Géodynamique et de Séismologie, volume 7, Luxembourg.
- Grünthal, G. (editor), 1998. *European Macroseismic Scale 1998 (EMS-98)*. European Seismological Commission, sub commission on Engineering Seismology, working Group Macroseismic Scales. Conseil de l'Europe, Cahiers du Centre Européen de Géodynamique et de Séismologie, volume 15, Luxembourg.
- Herrero A. & Bernard P., 1994. *A kinematic self-similar rupture process for earthquakes*. Bulletin of Seismological Society America. 84, 1216–1228.
- Hartzell S., Harmsen S., Frankel A. and S. Larsen (1999). Calculation of broadband time histories of ground motion: Comparison of methods and validation using strong-ground motion from the 1994 Northridge earthquake. *Bulletin of the Seismological Society of America*, 89, 6, 1484-1504.
- Housner G.W., 1952. *Intensity of ground motion during strong earthquakes. Second technical report*. August 1952, California Institute of Technology, Pasadena, California.
- Improta L., Bonagura M., Capuano P., Iannaccone G., 2003. *An integrated geophysical investigation of the upper crust in the epicentral area of the 1980, Ms=6.9, Irpinia earthquake (Southern Italy)*. Tectonophysics 361, 139-169.
- Khater M., Scawthorn C., Johnson J.J., 2003. *Loss estimation*. In Earthquake Engineering Handbook, W.Chen and C. Scawthorn (editors), CRC Press, Chapter 31.
- Lucantoni, A., Bosi, V., Brammerini, F., De Marco, R., Lo Presti, T., Naso, G., Sabetta, F., 2001. *Il rischio sismico in Italia*. Servizio Sismico Nazionale, Ingegneria Sismica, XVIII- -N. 1
- Mai, P.M. & G. C. Beroza, 2003. *A hybrid method for calculating near-source, broadband seismograms: application to strong motion prediction*. Physics of the Earth and Planetary Interiors, 137, 183-199.
- Marcellini A. & Paganì M., 2004. *Seismic zonation methodologies with particular reference to the Italian situation*. Recent Advances in Earthquake Geotechnical Engineering and Microzonation, A. Ansal (editor), Kluwer Academic Publisher, Printed in the Netherlands.

- Margaris, B.N. & Boore D. M., 1998. *Determination of $\Delta\sigma$ and k_0 from response spectra of large earthquakes in Greece*. Bulletin of Seismological Society of America, 88, 170-182.
- Margottini, C., Molin, D., and Serva, L., 1992. *Intensity versus ground motion: a new approach using Italian data*. Engineering Geology, 33, 45-58.
- Margottini C, Molin D, Narcisi B, Serva L., 1987. *Intensity vs. acceleration: Italian data*. In: Proceedings of workshop on historical seismicity of central-eastern Mediterranean region.
- Masi A., 2003. *Seismic vulnerability assessment of gravity load designed R/C frames*. Bulletin of Earthquake Engineering, Vol. 1, N. 3, pp. 371-395.
- Masi A., Vona M., Mucciarelli M., 2010. *Selection of natural and synthetic accelerograms for seismic vulnerability studies on RC frames*. Journal of Structural Engineering, ASCE Special Issue devoted to "Earthquake Ground Motion Selection and Modification for Nonlinear Dynamic Analysis of Structures". DOI: 10.1061/(ASCE)ST.1943-541X.209.
- McGuire R.K., 1995. *Probabilistic seismic hazard and design earthquakes: closing the loop*. Bulletin of Seismological Society of America. 85, 5, 1275-1284.
- McGuire R.K., 2001. *Deterministic vs. probabilistic earthquake hazards and risks*. Soil Dynamics and Earthquake Engineering, 21, 377-384.
- Medvedev J., 1962. *Engineering Seismology*. Akademia Nank Press, Moscow.
- Medvedev, S.V., 1977. *Seismic Intensity Scale M.S.K. – 76*. Publ. Inst. Geophys. Pol. Acad. Sc., A-6 (117), Warsaw.
- Molin D., 1995. *Consideration on the assessment of macroseismic intensity*. Annals of Geophysics. 38, 805-810.
- Mouroux P. & Le Brun B., 2006. *Risk-UE Project: An Advanced Approach to Earthquake Risk Scenarios with Application to Different European Towns*. In Assessing and Managing Earthquake Risk. Geo-scientific and Engineering Knowledge for Earthquake Risk Mitigation: developments, tools, techniques. Carlos Sousa Oliveira, Antoni Roca and Xavier Goula. Springer Netherlands Publisher. pp. 479 – 508.
- Mucciarelli M., Camassi R., Gallipoli M.R., 2002. *Collection of Macroseismic Data in a Digital Age: Lessons from the 1999 Kocaeli, Turkey Earthquake*. Bulletin of Seismological Society of America, 73, N.3, 325–331.
- NTC08, 2008. *D.M. 14 gennaio 2008 - Norme tecniche per le costruzioni*. Ministero delle Infrastrutture. Available at web site <http://www.cslp.it>.
- OPCM 3274, 2003. *Ordinanza del Consiglio dei Ministri n. 3274. Primi elementi in materia di criteri generali per la classificazione sismica del territorio nazionale e di normative tecniche per le costruzioni in zona sismica*. GU n. 72 giugno 2003. Available at web site <http://www.cslp.it>.
- Pacor F. & Mucciarelli M., 2007. *Scenari di Scuotimento in Aree di Interesse Prioritario e/o Strategico*. Progetto DPC-INGV S3. Available at web site <http://esse3.mi.ingv.it/index.php>
- Pacor F., Cultrera G., Mendez A. , Cocco M., 2005. *Finite Fault Modeling of Strong Ground Motion Using a Hybrid Deterministic - Stochastic Method*. Bulletin of Seismological Society of America. 95, 225-240.
- Pergalani F., Romeo R, Luzi L., Petrini V., Pugliese A, Sanò T., 1999. *Seismic microzoning of the area struck by Umbria–Marche (Central Italy) Ms 5.9 earthquake of 26 September 1997*. Soil Dynamics and Earthquake Engineering, 18, 279-296.
- RADIUS, 1999. *Risk Assessment Tools for Diagnosis of Urban Areas Against Seismic Disasters. Report United Nations Initiative towards Earthquake Safe Cities*. Available at web site <http://www.geohaz.org/projects/radius.html>
- Reiter L., 1990. *Earthquake Hazard Analysis*. Columbia University Press, New York, 254 pp.

Rovelli A., Bonamassa O., Cocco M., Di Bona M., and S. Mazza (1988) Scaling laws and spectral parameters of the ground motion in active extensional areas in Italy, *Bulletin of the Seismological Society of America*, 78; 2, 530-560

Sieberg A., 1930. *Geologie der Erdbeben*. Handbuch der Geophysik, 2, 4, pp. 550-555.

Valensise G., Pantosti D., Basili R., 2004. *Seismology and Tectonic Setting of the 2002 Molise, Italy, Earthquake*. *Earthquake Spectra*, 20, 23-37.

Working Group ITACA, 2008 - *Data Base of the Italian strong motion data*. Available at web site <http://itaca.mi.ingv.it>

Zollo A., Bobbio A., Emolo A. Herrero A. De Natale G., 1997. *Modelling of ground acceleration in the near source range: the case of 1976, Friuli earthquake (M= 6.5), northern Italy*. *Journal of Seismology*, 1, 305-319.

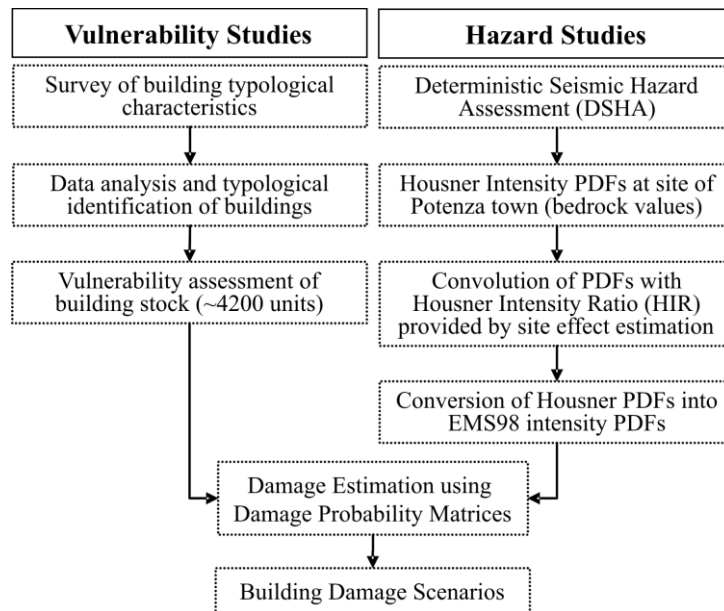


Figure 1. Flowchart of the adopted methodology.

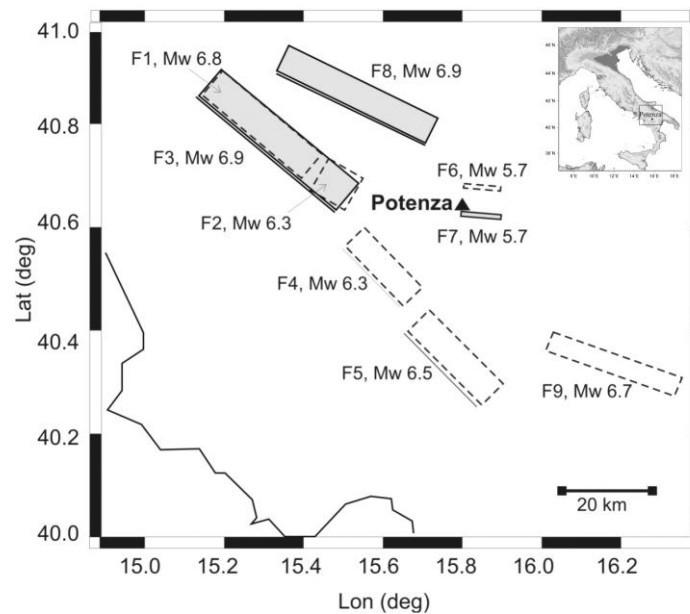


Figure 2. Map of the faults location with respect to Potenza. Refer to the Table 1 for the fault codes and names.

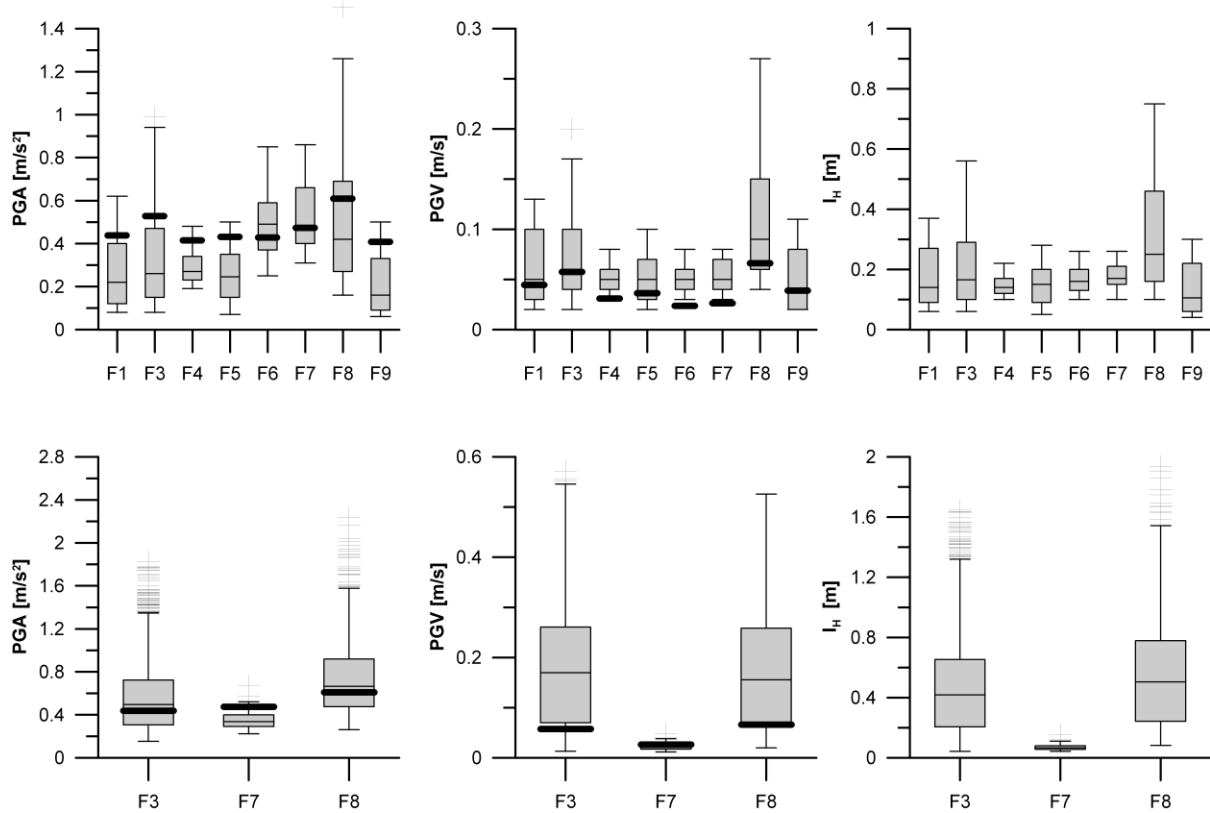


Figure 3. Top: Ground motions at level 1, computed by the DSM simulation method, experienced at Potenza. In the figures we show the geometrical mean between horizontal components of PGA (left), PGV (centre) and I_H (right), obtained for all rupture scenarios on each selected fault. Bottom: Ground motions at level 2, computed by the HIC method, experienced at Potenza town. Again, the geometrical mean between horizontal components of PGA (left), PGV (centre) and I_H (right), obtained for all rupture scenarios on each selected fault are shown in the figures. Each box encloses 50% of the data with the median value of the parameter displayed as a thin line; the top and the bottom of the box mark the limits of $\pm 25\%$ of the population; the lines extending from the top and the bottom of each box mark the minimum and the maximum values within the data (outliers excluded); the data that have values 1.5 times greater/lower than the top/bottom value of the box are called outliers (black crosses). The thick black lines are the median values of peak ground parameters estimated by the Italian Ground Motion Prediction Equation (ITA08, Bindi *et al.*, 2009).

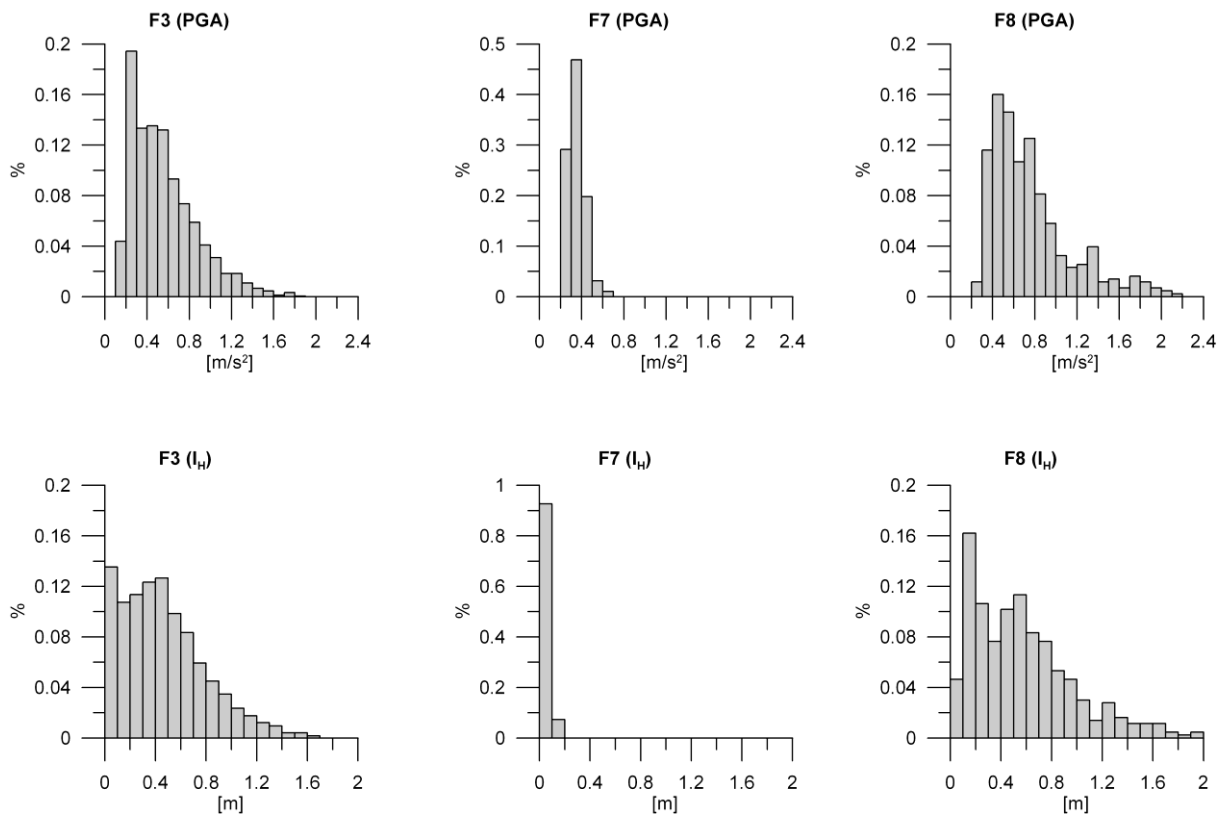


Figure 4. Histograms of PGA and I_H computed for all shaking scenarios at Potenza for F3, F7 and F8 faults. Each bin of the histogram is large $0.1 m/s^2$ for PGA and $0.1m$ for I_H .

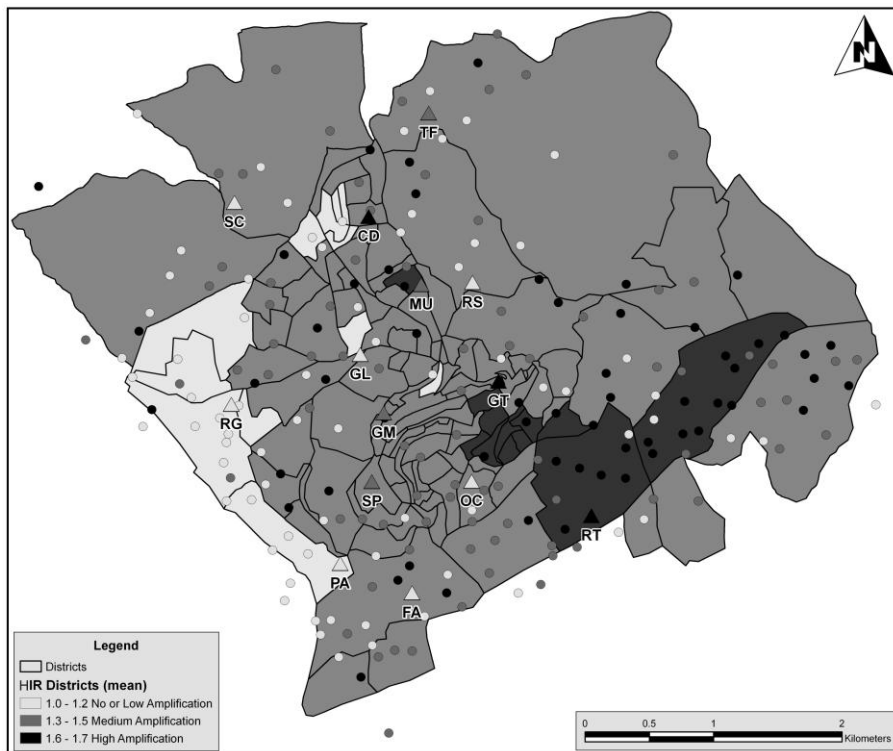


Figure 5. Seismic microzonation of urban area of Potenza town in terms of amplification coefficient OF Housner intensity (HIR). For cleanness of draw, the values of HIR have been summarized in three homogeneous amplification areas: no or low (HIR between 1.0-1.2), medium (HIR between 1.3-1.5) and high (HIR between 1.6-1.7). In the figure, the triangles represent the 14 long term monitoring stations while the circles are the 230 single station measurements (From Pacor & Mucciarelli, 2007).

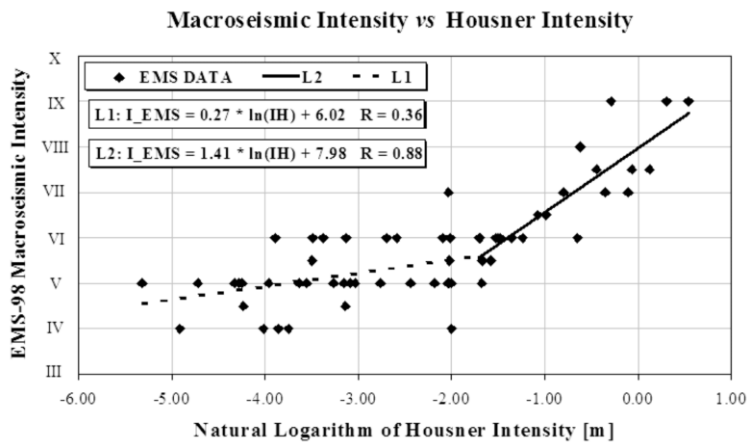


Figure 6. EMS intensities versus the natural logarithm of Housner intensity. The black continuous line represents the best fit curve obtained for Housner intensities larger than 0.18m while the dashed curve corresponds to the best fit for I_H lower than 0.18m.

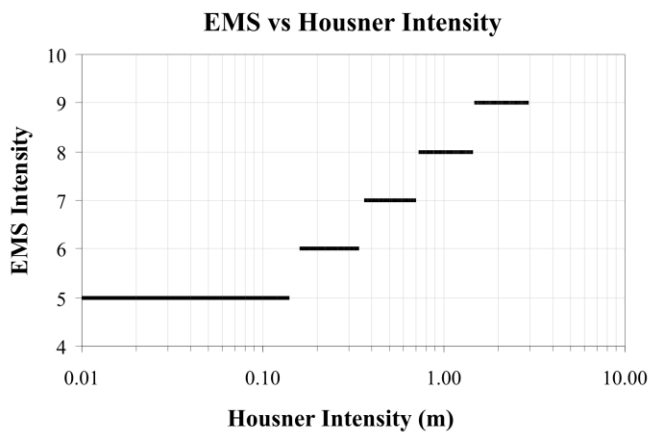


Figure 7. Macro seismic intensity (according to the EMS scale) with respect to the Housner intensity values. The I_H axes is in logarithmic scale.

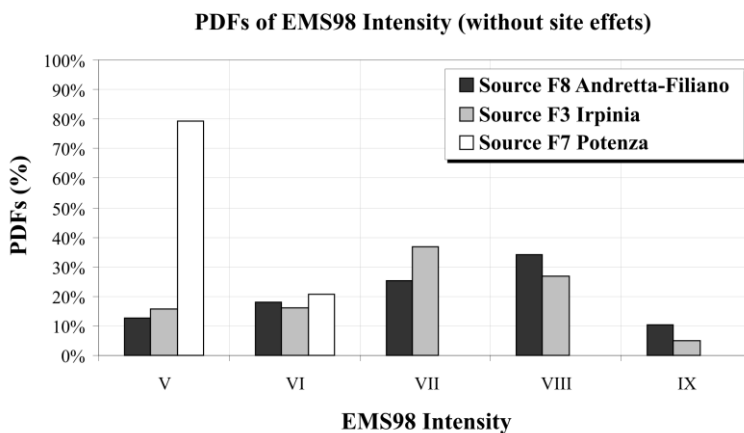


Figure 8. PDFs for the EMS98 intensity for the three shaking scenarios simulated for the sources F8, F7 and F3 without including the site effects.

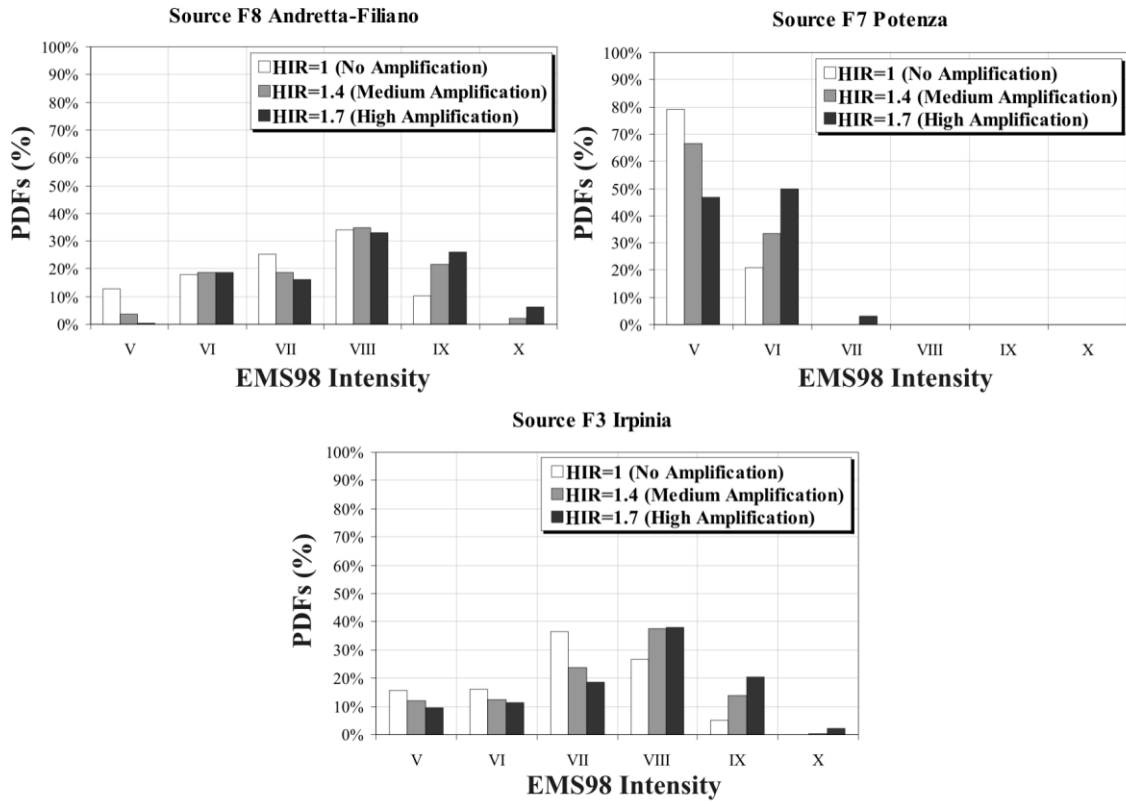


Figure 9. PDFs for the EMS98 intensity that include the site effects, distinct for the three shaking scenarios (sources F8, F7 and F3). In the figures are reported the results obtained using the soil amplification coefficients HIR=1, 1.4 and 1.7 (see text for more details).

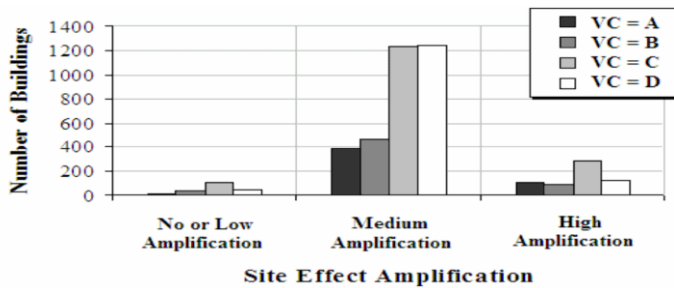


Figure 10. Buildings number for each vulnerability class (VC) and for each site zone (no or low amplification zone includes the area with HIR=1.0-1.2, medium amplification for areas with HIR=1.3-1.5, and high amplification for areas with HIR=1.6-1.7).

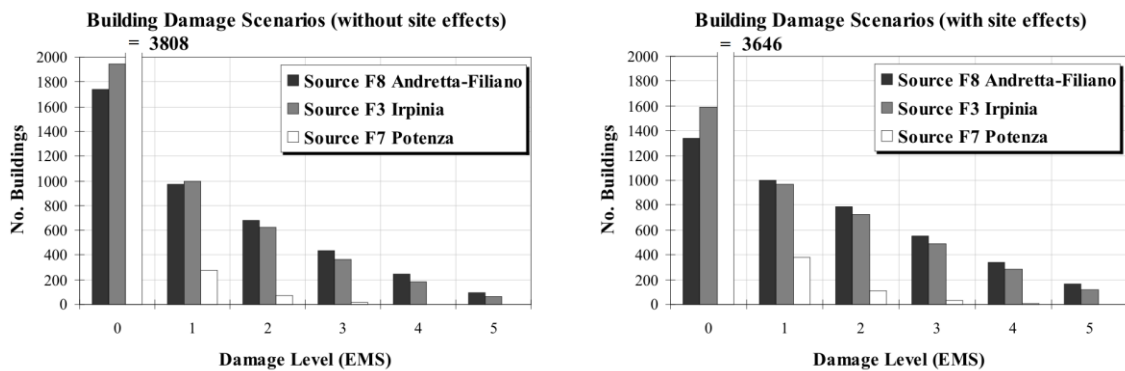


Figure 11. Damage distribution, in terms of number of buildings, obtained without including (left) and including (right) the site effects for the three earthquake scenarios associated to the faults F8, F7 and F3.

Fault code	F1	F2	F3	F4	F5	F6	F7	F8	F9
	ITGG077	ITGG078	ITGG007	ITGG010	ITGG008	ITGGa84	ITGGd84	ITG063	xxx
Fault name	Colliano	Irpiria	Irpiria	Melandro	Agri Valley	Potenza	Potenza	Andretta	Scorciabuoi
	Irpiria 0s	20s	0+20 s	Pergola				Filiano	
Strike (°)	310	300	310	317	316	95	95	296	110
Dip (°)	60	60	60	60	60	88	88	70	75
Rake (°)	270	270	270	270	270	175	175	230	270
Length (km)	28.0	9.0	38.0	17.9	23.0	7.9	7.9	35.0	30.0
Width (km)	15.0	15.0	15.0	11.3	13.5	6.2	6.2	18.0	16.0
Depth (km)	1.0	1.0	1.0	1.0	1.0	14.8	14.8	1.0	1.0
Ave.Slip (m)	1.65	0.70	1.40	0.57	0.74	0.24	0.26	1.3	0.87
Mw (*)	6.8	6.3	6.9	6.3	6.5	5.7	5.7	6.9	6.7
Distance (km)	32	18	23	19	23	5	1	16	33

Table 1. Geometrical and focal parameters of the reference seismogenic sources for Potenza. All data are taken from DISS v. 3.0.2, (DISS Working Group, 2006; Basili *et al.*, 2008) except that relative to the Scorciabuoi fault (see text for detail). The distance in the table is the fault distance to Potenza used to compute the peak ground motion values by Ground Motion Prediction Equations.

h (km)	Vp (km/s)	Vs=Vp/1.81 (km/s)	Qs	Rho (g/cm3)	Comments
0	3.5	1.93	100	2.3	
2	4.5	2.49	100	2.5	
4	5.7	3.15	100	2.6	Apula platform
10	6.5	3.59	100	2.7	
25	7.5	4.14	100	2.9	
35	8.1	4.48	100	3.2	Moho

Table 2. Crustal velocity model (after Amato & Selvaggi, 1993; Improta *et al.*, 2003). Here, h is the depth of the layer, V_P and V_S represent the velocity of the P- and S-waves, respectively. Rho is density and Q_S is the S-wave quality. The depths of the Apula Platform and of the Moho are also reported.

	Masonry	Reinforced Concrete	Other
No. Buildings	2351	1743	83
% of No. Buildings	56%	42%	2%
Volume [m ³]	2437876	8341135	161329
% of Volume	22%	76%	2%

Table 3. Distribution of the buildings, in terms of number and volume, with the respective percentages, for the most widespread building types. The term other includes all the buildings having a different typology from masonry and reinforced.

Building age	Masonry				Reinforced Concrete			
	No.	% No.	Vol. [m ³]	% Vol.	No.	% No.	Vol. [m ³]	% Vol.
<1919	222	5%	211816	2%	2	0%	6241	0%
1919-1945	280	7%	435666	4%	10	0%	17995	0%
1946-1960	430	10%	539408	5%	165	4%	853242	8%
1961-1971	436	10%	249426	2%	336	8%	1562062	14%
1972-1975	178	4%	91952	1%	158	4%	710298	6%
1976-1980	190	5%	157595	1%	295	7%	1527892	14%
1980-1990	205	5%	79670	1%	347	8%	865945	8%
>1990	0	0%	0	0%	213	5%	1386908	13%
Retrofitted buildings	408	10%	672343	6%	217	5%	1410549	13%

Table 4. Frequency distribution of the age of masonry and reinforced concrete buildings in terms of number and volume. The percentages have been computed on the total building number (as a result of rounding to integer values they may not sum to 100).

Horizontal Structure		Vertical Structure							
		Masonry Quality			Mixed	RC		Steel	Other
Bad	Medium	Good	Frame	Wall					
Vaults	Without tie-beams	A	A	A	B	---	---	---	---
	With tie-beams	A	A	A	B	---	---	---	---
Floors	Deformable	A	A	B	C	C	C	C	C
	Semirigid	B	B	C	C	C	C	C	C
	Rigid, RC	B	C	C	C	C	C	C	C
Building retrofitted after 1980					D				
Buildings built after 1980					D				

Table 5. Vulnerability classes according to building age and structural type (Braga *et al.*, 1982; Dolce *et al.*, 2003).

Horizontal Structure		Vertical Structure							
		Masonry Quality			Mixed	RC		Steel	Other
Bad	Medium	Good	Frame	Wall					
Vaults	Without tie-beams	33	8	5	2	---	---	---	---
	With tie-beams	3	2	0	0	---	---	---	---
Floors	Deformable	398	68	396	42	52	0	9	0
	Semirigid	83	17	209	21	44	0	26	0
	RC	107	31	249	77	857	16	0	6
Retrofitted structures after 1980					625				
Buildings built after 1980					791				

Table 6. Number of building for each building set belonging to the same vulnerability class.

	Vulnerability Classes			
	A	B	C	D
No. Buildings	517	605	1639	1416
% No. Buildings	13%	14%	39%	34%
Volume [m ³]	573543	506009	5382371	4478416
% Volume	5%	5%	49%	41%

Table 7. Distribution of buildings, in terms of number and volume, for each vulnerability class.

ID Source	Site Effects	Damage Level [EMS98]					
		Ld = 0	Ld = 1	Ld = 2	Ld = 3	Ld = 4	Ld = 5
F8	With	1340	996	786	550	338	164
	Without	1743	974	681	437	243	96
F7	With	3646	379	113	31	5	0
	Without	3808	274	70	19	3	0
F3	With	1594	971	722	485	282	121
	Without	1948	994	623	362	183	65

Table 8. Number of buildings for each EMS98 damage level. The results are shown for seismic scenarios obtained considering (with) and not considering (without) the site effects.

ID Source	Site Effects	Damage Level [EMS98]					
		Ld = 0	Ld = 1	Ld = 2	Ld = 3	Ld = 4	Ld = 5
F8	With	4.03	2.80	2.06	1.29	0.63	0.22
	Without	5.14	2.68	1.70	0.96	0.43	0.13
F7	With	10.04	0.78	0.17	0.04	0.01	0.00
	Without	10.39	0.52	0.10	0.02	0.00	0.00
F3	With	4.70	2.71	1.85	1.10	0.51	0.17
	Without	5.72	2.69	1.48	0.75	0.32	0.09

Table 9. Volume (million of m³) of buildings for each EMS98 damage levels. Comparison between the results of seismic damage scenarios obtained with and without site effects.

ID Source	Site Effects	DI _{med}
F8	with	0.45
	w/o	0.42
F7	with	0.27
	w/o	0.26
F3	with	0.43
	w/o	0.39

Table 10. Mean damage index (DI_{med}) for the three earthquake shaking scenarios (source F8, F7 and F3) with and without site effects.

ID Source	Site Effects	Percentage of unusable buildings	
		Considering the number	Considering the volume
F8	with	17 %	12 %
	w/o	12 %	8 %
F7	with	0.5 %	0.2 %
	w/o	0.2 %	0.1 %
F3	with	14 %	10 %
	w/o	10 %	6 %

Table 11. Percentages of unusable buildings for the damage scenarios obtained for earthquakes occurring on the F8, F7 and F3 fault. The results are presented including (with) and not including (without) the site effects.